

# Principal Component Analysis of Dual-luminophore Pressure/Temperature Sensitive Paints

Carroll, B. F.\*<sup>1</sup>, Hubner, J. P.\*<sup>1†</sup>, Schanze, K. S.\*<sup>2</sup> and Bedlek-Anslow, J. M.\*<sup>2</sup>

\*1 Department of Aerospace Engineering, Mechanics & Engineering Science, University of Florida, Gainesville, FL 32611-6250, U.S.A.

\*2 Department of Chemistry, University of Florida, Gainesville, FL 32611, U.S.A.

Received 10 November, 2000.

Revised 19 February, 2001.

**Abstract:** Multi-luminophore pressure/temperature sensitive paints are investigated using principal component analysis of the spectral emission from the coatings. Two formulations are investigated. The first consists of Ru (4,7-diphenylphenanthroline) dichloride (Ruphen) and Coumarin-7 luminophores. The second coating contains Pt(II) meso-tetrakis (pentafluorophenyl) porphine (PtTFPP) and diethyloxadicyanone iodide (DOCI). The principal component analysis revealed that the Ruphen/Coumarin-7 coating requires three fundamental spectra or modes to adequately model the coating emission characteristics. The PtTFPP/DOCI coating was modeled adequately with only two modes. Analysis of the PtTFPP/DOCI coating also revealed that a temperature independent calibration of the pressure sensing function could be developed. The requirement for a wind-off reference image was also eliminated.

**Keywords:** pressure sensor, temperature sensor, luminescent coating.

## 1. Introduction

Pressure and Temperature Sensitive Paints, PSP and TSP, are luminescent coatings for which the luminescence intensity varies with pressure and temperature, respectively. As has been well documented in the literature, PSP coatings also display undesirable temperature sensitivities (Schanze et al., 1997) which can cause significant errors in the pressure determination. Various techniques to correct for the temperature effects exist (Bencic, 2000; Hubner et al., 1997; Woodmansee and Dutton, 1998); however, the temperature field must be measured concurrently with the pressure field to implement these corrections. Increasing interest has been placed on the development of multi-luminophore coatings that provide spectrally resolved indications of pressure, temperature and/or reference intensity. A new technique of PSP/TSP data analysis based on principal component analysis (alternately called proper orthogonal decomposition) was recently introduced by Carroll et al. (1999). This current work presents further developments of the principal component approach for implementing temperature corrections for dual-luminophore pressure/temperature sensitive paints.

## 2. Chemical Formulations

Two dual-luminophore coatings are considered in this study. The first consists of Ru (4,7-diphenylphenanthroline) dichloride (Ruphen) as the oxygen sensing luminophore and Coumarin-7 as the temperature sensing luminophore. The two luminophores were dispersed in a polydimethylsiloxane (PDMS)

---

† Joint appointment with AeroChem Corporation

polymer binder. This coating was applied without a primer layer. The second coating consisted of Pt(II) meso-tetrakis (pentafluorophenyl) porphine (PtTFPP) as the oxygen sensing luminophore and diethyloxadicyanone iodide (DOCI) absorbed microspheres produced via precipitation polymerization as the temperature sensing luminophore distributed in a vinyl polydimethylsiloxane (VPDMS) polymer binder. A primer layer of 800 TiO<sub>2</sub> in silanol terminated polydimethylsiloxane (SPDMS) was used as a primer layer.

### 3. Principal Component Analysis

The data analysis procedure utilized in this study is based on principal component analysis of the spectral distributions from the coatings (Carroll et al., 1999). A spectrally resolved data matrix is obtained from a spectrophotometer. Alternately the data may be obtained from a CCD camera using a series of optical filters with each pixel on the CCD supplying spectral data for a single environmental condition (i.e. pressure and temperature condition). Thus the data matrix may be expressed as

$$\mathbf{S} = S_{ln} \quad (1)$$

where  $\mathbf{S}$  is a two dimensional array of measured intensities,  $l$  is the wavelength and  $n$  is the environmental condition specifying a pressure/temperature combination. The columns of  $\mathbf{S}$  give the spectral distribution of each pixel of a camera image or each environmental condition for a pointwise spectrophotometer measurement. We make the assumption that  $\mathbf{S}$  may be represented by the product of a principal component array,  $\mathbf{F}$ , and a contributions array,  $\mathbf{A}$ ,

$$\mathbf{S} = S_{ln} = \mathbf{F}\mathbf{A} = F_{lk}A_{kn}. \quad (2)$$

In this expression,  $k$  is the number of factors or modes used to represent the complete data set,  $\mathbf{S}$ . Thus, our goal is to generate a reduced order model with  $k$  important factors used to represent  $\mathbf{S}$ . The principal component array,  $\mathbf{F}$ , would be the fundamental luminescence spectra and  $\mathbf{A}$  would be an attenuation multiplier that accounts for variations in environmental parameters (i.e. pressure, temperature, etc.).

The next steps in the analysis follow the approaches outlined by Lawton and Sylvestre (1971), Malinowski and Howery (1980) and Sun et al. (1987). The data matrix,  $\mathbf{S}$ , is normalized such that for each value of  $n$  the sum over  $l$  yields unity. This is done to avoid numerical problems with the matrix manipulations. The normalization also eliminates the need of forming a ratio of the data to a reference condition. Removing the need for a wind off reference can be very beneficial, especially in large wind tunnel facilities where on/off cycles are time consuming. A covariance matrix,  $\mathbf{Z}$ , is defined by

$$\mathbf{Z} \equiv \mathbf{S}\mathbf{S}^T. \quad (3)$$

The covariance matrix is then diagonalized by finding a matrix,  $\mathbf{V}$ , such that

$$\mathbf{V}^{-1}\mathbf{Z}\mathbf{V} = \mathbf{E}. \quad (4)$$

A solution to Eq. (4) is easily obtained using a standard eigenvector solver. The columns of  $\mathbf{V}$  are mutually orthogonal eigenvectors and the diagonal elements of  $\mathbf{E}$  are the eigenvalues (off diagonal elements of  $\mathbf{E}$  are zero). Making use of the orthogonality of  $\mathbf{V}$  (i.e.  $\mathbf{V}^T = \mathbf{V}^{-1}$ ) one can show that

$$\mathbf{A} = \mathbf{V}^T\mathbf{S} \quad (5)$$

and

$$\mathbf{F} = \mathbf{V}. \quad (6)$$

The product  $\mathbf{F}\mathbf{A}$  is an abstract model for the data matrix  $\mathbf{S}$  in that it does not necessarily represent the data in any physically meaningful format. Also note that since the problem has been overdetermined, the eigenvectors,  $\mathbf{V}$ , contain extraneous data corresponding to noise. However, the eigenvectors that correspond to the largest

eigenvalues contain the "important" information. Stated another way, each eigenvector represents an abstract factor that models the variance of the spectral data set. A large eigenvalue indicates the corresponding eigenvector is an important contribution to the data while a small eigenvalue indicates the corresponding eigenvector is unimportant. By neglecting unimportant eigenvectors we achieve a mathematically compact representation of the data. For example, a two factor (or two mode) reconstruction is obtained by setting  $k = 2$  in Eq. (2) and nulling the appropriate matrix elements in Eqs. (5) and (6). We will refer to the reconstructed or compressed model for  $\mathbf{S}$  as  $\mathbf{S}'$  which for  $k = 2$  is given by

$$\mathbf{S}' = S'_{in} = F_{ik}A_{kn} = F_1(I)A_1(n) + F_2(I)A_2(n). \quad (7)$$

Note that the data set  $\mathbf{S}'$  is still a  $l$  by  $n$  matrix but  $\mathbf{F}$  and  $\mathbf{A}$  have been reduced in size from Eqs. (5) and (6). One should remember that the attenuation multipliers are functions of environmental conditions as determined by the pressure-temperature pair. Accordingly, we may think of  $A_1$  and  $A_2$  as functions of pressure and temperature, i.e.  $A_1(n) = A_1(P, T)$  and  $A_2(n) = A_2(P, T)$ . Calibration of the coating is achieved by obtaining the functional forms of  $A_1$  and  $A_2$ . Various procedures exist to rotate or transform the eigenvectors in such a way as to extract physically important information from the data set (Carroll et al., 1999; Saltiel et al., 1994). The transformation process may also be applied to optimize the compressed model for calibration purposes, i.e. a transformed representation may be sought that minimizes temperature dependencies in one of the calibration functions.

## 4. Results and Discussion

The environmental conditions (i.e. pressure-temperature conditions) for this series of tests are listed in Tables 1 and

Table 1. Environmental conditions for Ruphen/Coumarin-7.

Temperature (K)	Pressure (kPa)
276	0.21
276	14.2
276	34.4
276	63.6
276	99.9
289	0.21
289	2.06
289	34.4
289	63.6
289	99.9
298	0.21
298	14.2
298	34.4
298	63.6
298	99.9
307	0.03
307	14.2
307	34.4
307	63.6
307	99.9

Table 2. Environmental conditions for PtTFPP/DOCI.

Temperature (K)	Pressure (kPa)
273	0.34
273	14.2
273	28.6
273	42.7
273	57.7
273	69.3
273	100.7
283	0.34
283	14.2
283	27.9
283	55.9
283	70.1
283	100.6
293	0.34
293	13.9
293	42.0
293	55.1
293	69.4
293	100.6
303	0.48
303	15.4
303	27.8
303	43.6
303	55.9
303	100.5

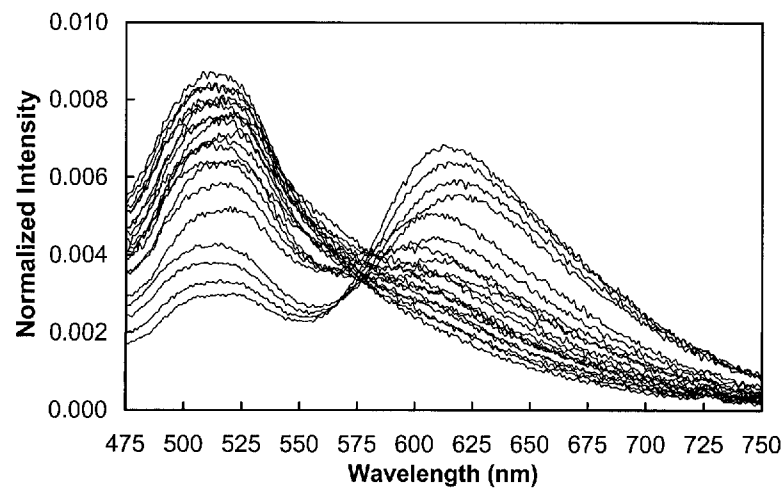


Fig. 1. Ruphen/Coumarin-7 normalized spectra for the environmental conditions listed in Table 1.

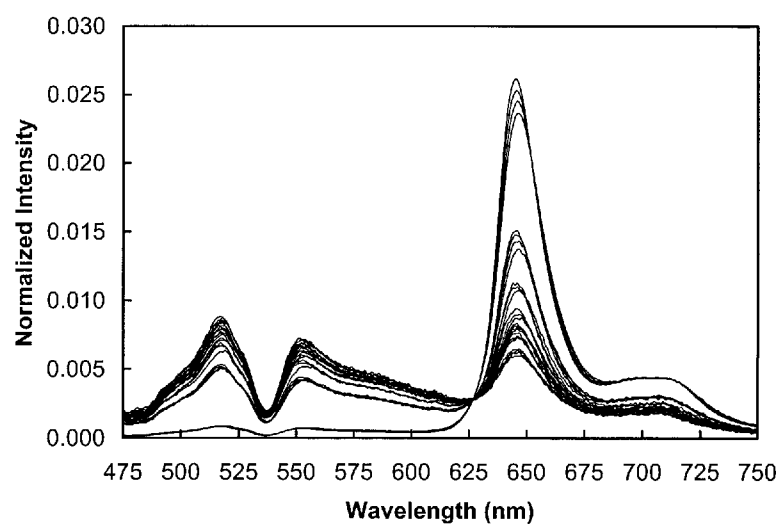


Fig. 2. PtTFPP/DOCI normalized spectra for the environmental conditions listed in Table 2.

2 for the Ruphen/Coumarin-7 and PtTFPP/DOCI coatings, respectively. Data for the luminescence spectral distribution of the coatings are shown in Figs. 1 and 2. This data was obtained with a SPEX F-112 fluorescence spectrophotometer. The luminescence signal for each environmental condition has been normalized by the area under the curve for that environmental condition. This effectively removes the need for a "wind-off" reference. In Fig. 1, the Ruphen dye displays a broad emission, centered around 620 nm, that depends on both pressure and temperature. The Coumarin-7 emission, centered at about 520 nm, is predominately sensitive to temperature with only weak pressure dependence. In Fig. 2, the PtTFPP is observed to have a much narrower emission than the Ruphen dye. This emission is sensitive to pressure and temperature. The DOCI emission in the green portion of the spectra is sensitive predominately to temperature.

The principal component analysis discussed above was applied to the two data sets. The abstract factors or fundamental spectra,  $F(i)$ , for the PtTFPP/DOCI coating are shown in Fig. 3 for the first three modes,  $F_1$ ,  $F_2$  and  $F_3$ . Mode 1 represents the general shape of the spectral distribution. Mode 2 gives a relative weighting between the temperature sensing dye (lower wavelengths) and the pressure/temperature sensing dye (higher wavelengths). Notice that  $F_2$  is negative for the lower wavelengths and positive for higher wavelengths, allowing the adjustment in the relative weighting. Mode 3 represents wavelength shifts in the spectra such as the wavelength dependence of the spectral peaks and valleys. Combining the fundamental spectra according to Eq. (7) we obtain reconstructed spectra as shown in Figs. 4-6. Three modes are required to accurately reconstruct the Ruphen/Coumarin-7 coating (Figs. 4 and 5), but only two modes are necessary to give a reasonable representation for the PtTFPP/DOCI formulation (Fig. 6). We see that the Ruphen/Coumarin-7 coating has significant wavelength shifts that require the third mode for accurate reproduction, even though the relative strength of the associated third eigenvalue is less

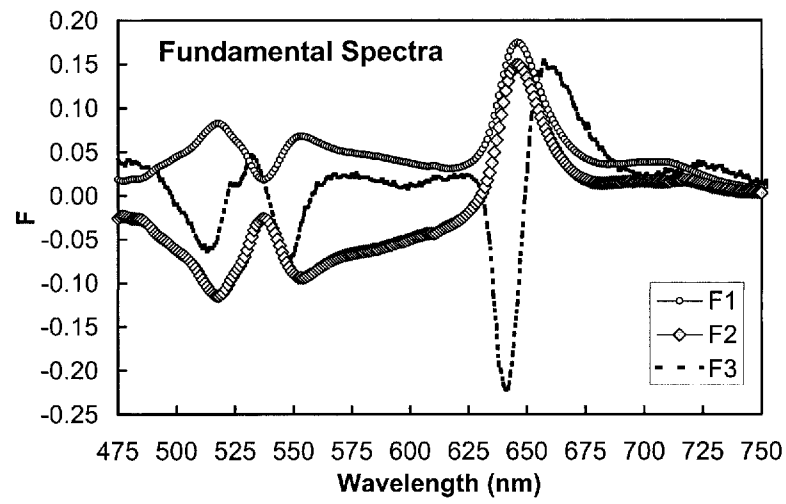


Fig. 3. Fundamental spectra from principal component analysis of the PtTFPP/DOCl coating.

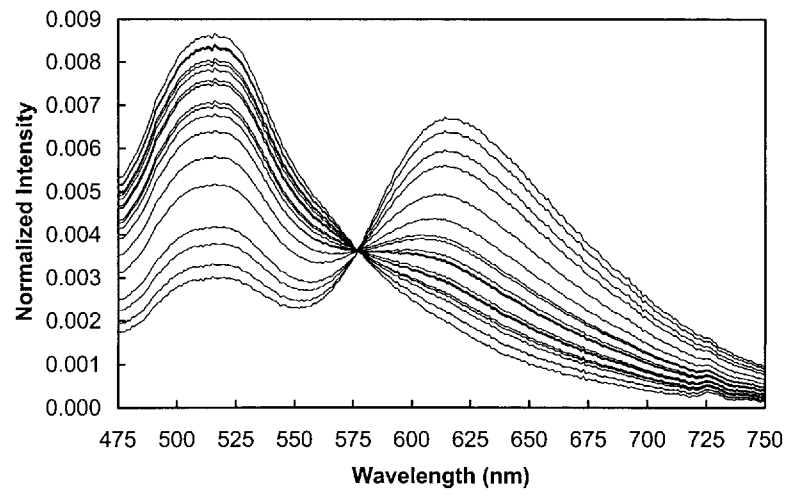


Fig. 4. Reconstructed spectra for Ruphen/Coumarin-7 using two modes.

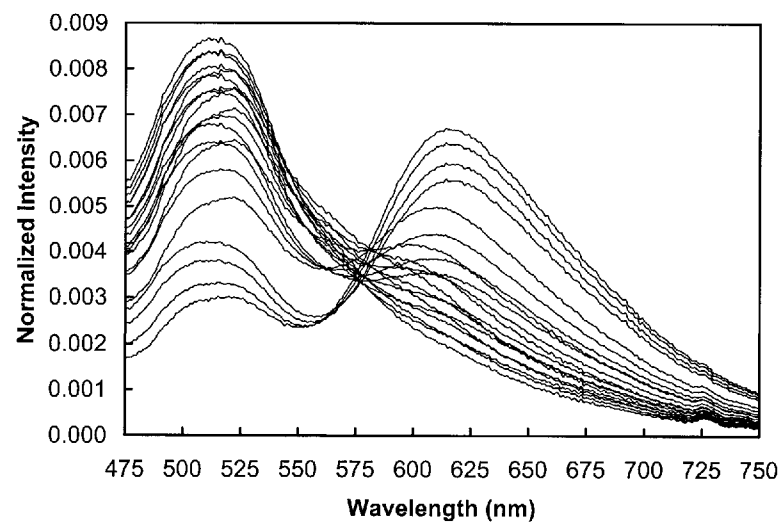


Fig. 5. Reconstructed spectra for Ruphen/Coumarin-7 using three modes.

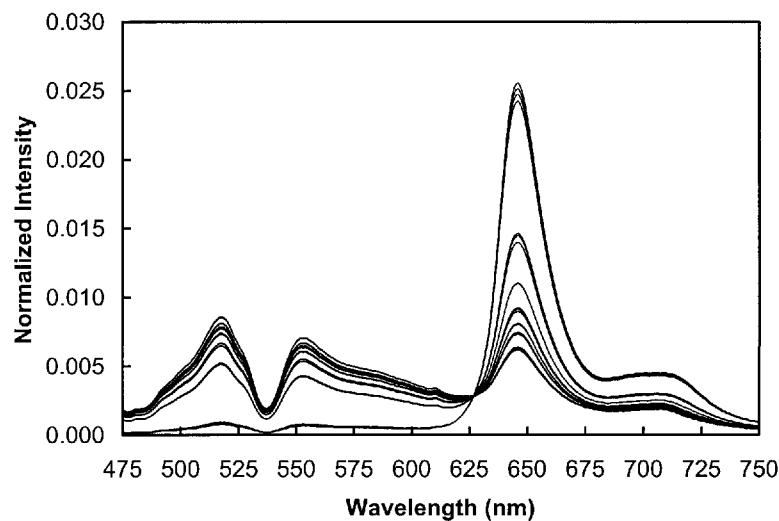


Fig. 6. Reconstructed spectra for PtTFPP/DOCI using 2 modes.

than 1% of the total system variance. When using only two modes, the Ruphen/Coumarin-7 reconstructed spectra has an isobestic point at approximately 575 nm which is not observed in the original spectra. In contrast, the PtTFPP/DOCI, which has much weaker wavelength shifts in the spectra, displays an isobestic point near 625 nm in the original spectra and the two mode reconstruction. The presence of an isobestic point in the original PtTFPP/DOCI data set (Fig. 2) indicates that molecular level interactions between the luminophores are not significant. This is consistent with the physical separation of the luminophores in the micro-encapsulated PtTFPP/DOCI formulation.

While molecular interactions between luminophores appear to be minimized in the PtTFPP/DOCI formulation, optical coupling between the luminophores is observed. This is evidenced by the optical bleaching at approximately 540 nm in Figs. 2 and 6. The PtTFPP exhibits several absorption bands. The first band is an intense near-UV band termed the Soret band at 395 nm. The second two bands appear in the visible region between 505 to 540 nm and are referred to as the Q bands. The emission of the DOCI-adsorbed microspheres is centered at 510 nm. Thus, the PtTFPP Q bands can absorb light from the DOCI emission band. The position of the PtTFPP probe relative to the microspheres in the PtTFPP/DOCI formulation was determined using a fluorescence microscope with the results shown in Fig. 7. Three images were obtained with a 40X objective (image size of 218  $\mu\text{m} \times 173 \mu\text{m}$ ) and 425 nm - 40 nm FWHM bandpass filter in front of the excitation source. Three emission filters, 630 nm - 60 nm FWHM bandpass, 525 nm - 50 nm FWHM bandpass and 475 nm longpass were used. Image C gives the combined emission, Image B gives the DOCI emission, and Image A depicts only the emission of the PtTFPP luminophore. The locations of the DOCI microspheres is apparent in Image B. In Image A, we see an intensity in the PtTFPP luminophore that is higher than that occurring away from the microspheres. This high intensity occurs at the microsphere locations identified in Image B and is caused by the "pumping" of the PtTFPP by the DOCI through optical energy transfer.

Turning attention back to the principal component results, we find that a convenient way to visualize the

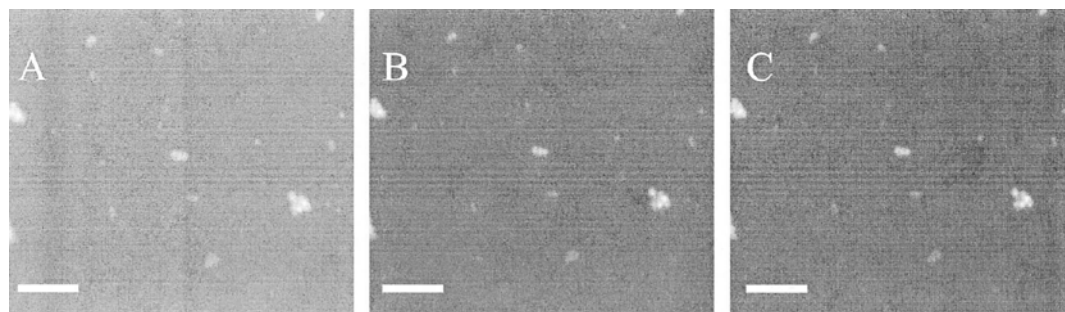


Fig. 7. Fluorescence images of the PtTFPP/DOCI using various emission filters. White scale bar is 37.9  $\mu\text{m}$  long. (A) 630 nm bandpass, (B) 525 nm bandpass, (C) 475 nm longpass.

characteristics of the coatings is by plotting the attenuation multipliers,  $A_1$  vs  $A_2$  as done in Fig. 8 for the PtTFPP/DOCI coating. Since  $A_1$  and  $A_2$  are functions of the environmental conditions, the  $A_1$ - $A_2$  plane represents all possible pressure/temperature pairs. Isotherms are drawn in Fig. 8. Considering Table 2, we see that the groupings of data points correspond roughly to lines of constant pressure. Thus for the PtTFPP/DOCI coating, the  $A_2$  parameter is nearly temperature independent, i.e. the isobars are approximately perpendicular to the  $A_2$  axis. For this particular coating formulation, the ratio  $A_2/A_1$  is also nearly temperature independent as is seen in Fig. 9. The open symbols in Fig. 9 correspond to the data in Table 2. Three additional data "test" points were also collected and are listed in Table 3. The solid curve in Fig. 9 is a fifth order polynomial curve fit to the original data set, given by

$$P_{cal} = -163.5 \left( \frac{A_2}{A_1} \right)^5 + \left( \frac{A_2}{A_1} \right)^4 - 105.1 \left( \frac{A_2}{A_1} \right)^3 + 56.75 \left( \frac{A_2}{A_1} \right)^2 - 57.99 \left( \frac{A_2}{A_1} \right) + 19.71. \quad (8)$$

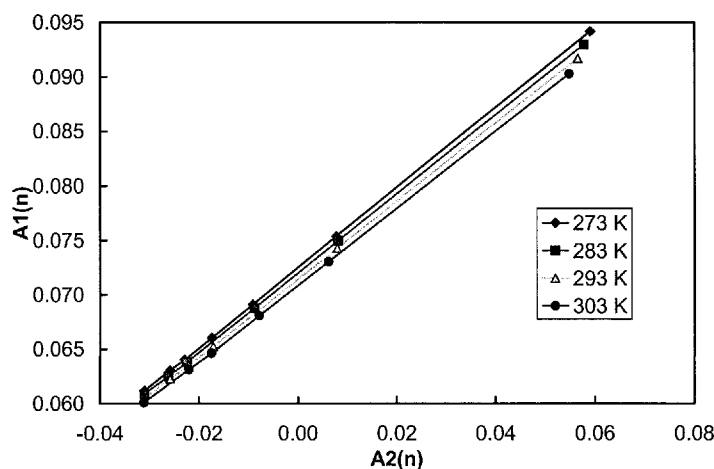


Fig. 8. Attenuation multipliers for the PtTFPP/DOCI coating. Isotherms are drawn. Isobars are approximately vertical lines indicating little temperature dependence in  $A_2$ .

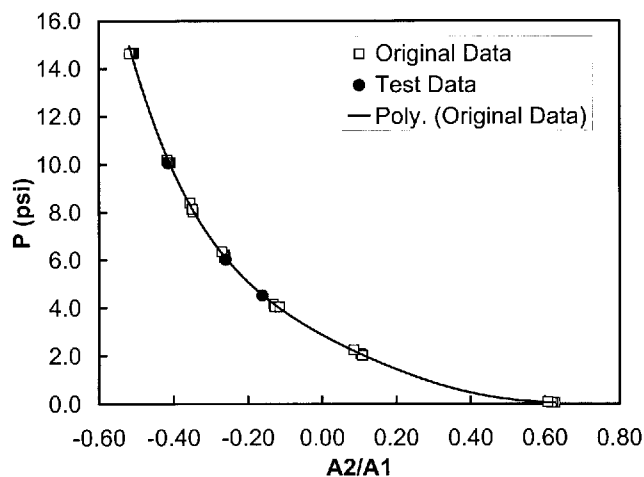


Fig. 9. Fifth order polynomial calibration curve that is independent of temperature. The three test data points were omitted from the principal component analysis to confirm the predictive ability of the calibration procedure.

The form of the curve given by Eq. (8) is similar to the inverse intensity response with respect to pressure observed in conventional Stern-Volmer PSP calibration functions. A calibration curve could also have been formulated in terms of just  $P$  vs  $A_2$ , however the functional form was not as simple. The calibration function, Eq. (8), has the advantage of being independent of temperature. In Table 3, a comparison is made between the true test point pressure,  $P_{me}$ , and the polynomial calibration,  $P_{cal}$ . To make the comparison, the principal component analysis was

Table 3. Calibration function verification.

$T$ (K)	$P_{true}$ (kPa)	$P_{cal}$ (kPa)	Rel. Error (%)
283	41.4	41.8	0.97
293	31.1	31.2	0.32
303	69.1	70.0	1.30

applied to the three test spectra and attenuation multipliers  $A_1$  and  $A_2$  were determined. These were then used in Eq. (8) to predict the pressure level. The error between the predicted and true pressure ranged from 0.32% to 1.30% of reading. One should also note that a coordinate rotation in the  $A_1$ - $A_2$  space would allow the temperature independent quality to be recast in terms of  $A_1$  only or  $A_2$  only, instead of the ratio  $A_2/A_1$ . Other coordinate rotations can be made to recast the fundamental spectra in terms of physically realistic processes (Stern-Volmer relation for the PtTFPP and an Arrhenius expression for the DOCI).

The ability to form a temperature independent calibration function for the PtTFPP/DOCI coating does not appear to be a universal property of multi-luminophore formulations. Figure 10 is a plot of  $A_1$  vs  $A_2$  for the Ruphen/Coumarin-7. This data set differs from that for the PtTFPP/DOCI (Fig. 8) in two main ways. For the Ruphen/Coumarin-7, the isobars are almost parallel to the isotherms. This makes it difficult to isolate the pressure dependence in a single attenuation multiplier, i.e. in  $A_1$  or  $A_2$ . The Ruphen/Coumarin-7 data also has a greater tendency to collapse to a single curve. When this occurs,  $A_1$  and  $A_2$  are not independent, requiring a third mode to decouple pressure and temperature.

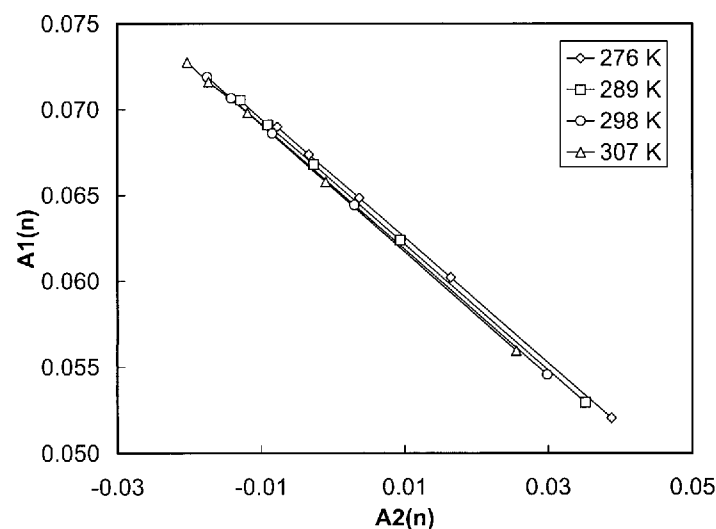


Fig. 10. Attenuation multipliers for the Ruphen/Coumarin-7 coating. Isotherms are drawn. Isobars are nearly parallel to the isotherms. It is difficult to decouple the pressure and temperature effects in  $A_1$  and  $A_2$ .

## 5. Conclusions

A data analysis procedure based on principal component analysis has been applied to two types of dual-luminophore pressure/temperature sensitive coatings. The spectral luminescent data was collected for a range of pressure and temperature conditions. The data was modeled by a weighted sum of two or three fundamental spectra. The weighting factors or attenuation multipliers are functions of the pressure/temperature conditions and can be used as calibration functions for the coatings. For the PtTFPP/DOCI coating, a temperature independent calibration function for pressure was easily obtained. However, for the Ruphen/Coumarin-7 coating, it was more difficult to decouple the pressure and temperature effects. This approach to PSP/TSP data analysis is promising since it has the potential to eliminate wind-off reference requirements. It also has the potential to automate temperature correction procedures for PSP measurements. Further work needs to be performed to determine the effect of bandpass filtering of the spectral data and spectral leakage in the filtering process. The suitability of the principal component analysis for in-situ calibration needs to be determined and the impact of variations in coating preparation, application and photodegradation on the principal component analysis also needs to be explored.



## References

- Bencic, T., Temperature Correction for Pressure-Sensitive Paint, NASA Tech Briefs, Jan, (2000), 50-51.
- Carroll, B. F., Hubner, J. P., Schanze, K. S., Bedlek, J. and Morris, M., Pressure and Temperature Measurements with a Dual-Luminophore Coating, 18th ICIASF Record (Toulouse, France, June 13, 1999), 18.1-18.8.
- Hubner, J. P., Carroll, B. F. and Schanze, K. S., Temperature Compensation Model for Pressure-Sensitive Paint, FEDSM97-3470, ASME Fluids Engineering Division Summer Meeting, (Jun. 1997).
- Lawton, W. H. and Sylvestre, E. A., Self Modeling Curve Resolution, *Technometrics*, 13 (1971), 617-633.
- Malinowski, E. R. and Howery, D. G., *Factor Analysis in Chemistry*, (1980), John Wiley & Sons, New York.
- Saltiel, J., Sears, Jr., D. F., Choi, J. O., Sun, Y. P. and Eaker, D. W., Fluorescence, Fluorescence-Excitation, and Ultraviolet Absorption Spectra of trans-1-(2-Naphthyl)-2-phenylethene Conformers, *Journal of Physical Chemistry*, 98 (1994), 35-46.
- Schanze, K. S. Carroll, B. F., Korotkevitch, S. and Morris, M. J., Temperature Dependence of Pressure Sensitive Paints, *AIAA Journal*, 35-2 (Feb. 1997), 306-310.
- Sun, Y. P., Sears, D. F. and Saltiel, J., 3-Component Self-Modeling Technique Applied to Luminescence Spectra, *Analytical Chemistry*, 59-20 (1987), 2515-2519.
- Woodmansee, M. A. and Dutton, J. C., Treating Temperature-Sensitivity Effects of Pressure-Sensitive Paint Measurements, *Experiments in Fluids*, 24 (1998), 163-174.

## Author Profile



Bruce F. Carroll: He received his B.S. degree in Mechanical Engineering from Texas A&M University in 1982 and his Ph.D. in Mechanical Engineering from the University of Illinois at Urbana-Champaign in 1988. He is currently an Associate Professor in the Department of Aerospace Engineering, Mechanics and Engineering Science at the University of Florida. His research interests include optical flow diagnostics applied to compressible and incompressible flows.



James Paul Hubner: He received his B.S. degree in Aerospace Engineering from the University of Florida in 1990 and his Ph.D. in Aerospace Engineering from the Georgia Institute of Technology in 1995 as an Office of Naval Research Graduate Fellow. He is currently the chief research engineer of AeroChem Corporation, a small engineering consulting company, and an adjunct assistant professor in the Department of Aerospace Engineering, Mechanics & Engineering Science at the University of Florida. His research and teaching interests are in experimental fluid and solid mechanics and more recently have focused on luminescent-based measurement techniques.



Kirk S. Schanze: He received his B.S. degree in Chemistry from Florida State University in 1979 and his Ph.D. in Physical Organic Chemistry from the University of North Carolina at Chapel Hill in 1984. He then spent a 2 year period as a Miller Fellow at the University of California at Berkeley before joining the Faculty of the Chemistry Department at the University of Florida in 1986. He is currently a Professor of Chemistry at UF and his research interests focus on the optical properties of organic and organometallic materials.



Joanne Bedlek-Anslow: She received her B.S. degree in Chemistry from Loyola University in Chicago in 1995. After spending a year in Italy studying Italian, Joanne began her graduate studies in Chemistry at the University of Florida. She completed her Ph.D. degree in 1999 with an emphasis on materials organic chemistry. She is currently working as a staff scientist at DuPont company in Columbia, SC. Her research interests are in the area of photoluminescence of materials with applications to temperature and pressure sensitive paints.